

## **Analysis of a Case History Involving a Concrete Slab Placed on an Expansive Soil**

Delwyn G. Fredlund and Hung Q. Vu

### ***Abstract***

The case history involves the analysis of a slab-on-ground placed on a thin layer of gravel over highly plastic clay. A subsurface investigation was undertaken prior to construction and one-dimensional oedometer tests were performed to measure the swelling pressures and the swelling index of the soil. The site was instrumented with a neutron moisture tube and ground movement gauges were installed at various depths. Approximately one year after construction, a water line burst below the slab and water gained access to the highly plastic clay. Over a short period of time the floor slab rose about 10 cm.

This paper presents two-dimensional numerical simulations of the site. The method of analysis is based on the general theory of unsaturated soils using two independent stress state variables. The results of the analysis were found to agree well with the measured data in terms of both total vertical displacements and final water contents. Parametric study results also showed the effect of measured soil parameters (i.e., swelling index and initial void ratio) and assumed parameters (i.e., Poisson's ratio and the coefficient of earth pressure at-rest) to the calculated displacements.

### ***Introduction***

The prediction of heave in unsaturated, expansive soils has been studied primarily as a one-dimensional type analysis. The available methods for the prediction of heave generally make use of the linear relationship between void ratio (or vertical strain) and the logarithms of net normal stress or soil suction. These approaches can be divided into methods based upon the stress path followed in the analysis (i.e., actual stress path or total stress path, Figure 1). The methods that are followed actual stress path, based on matric suction measurements, require the determination of soil suction and the measurement (or estimation) of the soil property relating a change in soil suction to volume change. The primary difficulties associated with these methods are related to the

accuracy of soil suction measurements and appropriate soil property (i.e., volume change index with respect to changes in matric suction,  $C_m$ ). The methods that follow a total stress path make use of the results from one-dimensional oedometer tests (i.e., the swelling index with respect to changes in net normal stress,  $C_s$ , and swelling pressure). The oedometer methods are used in many countries because soil suction measurements are not required and the soil properties (i.e., swelling index,  $C_s$ ) can more readily and accurately be measured (Fredlund and Rahardjo 1993). One disadvantage associated with of the oedometer-based methods is the difficulty in measuring a unique swelling pressure since it is sensitive to the testing procedure. The ability to accurately measure volume changes in a highly fissured and fractured soil is a limitation affecting all methods (or stress paths).

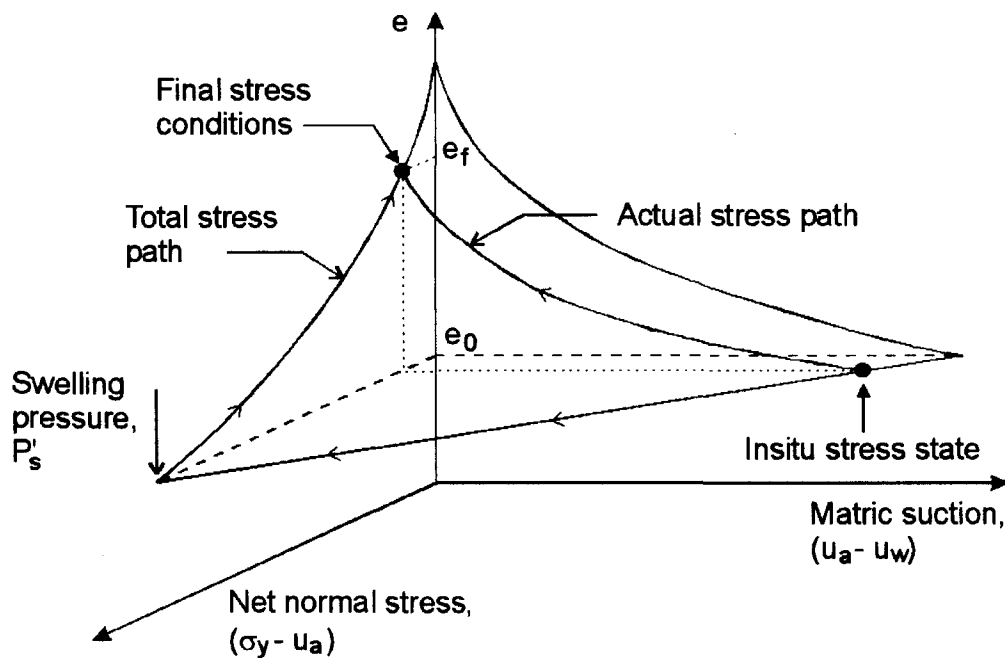


Figure 1. Stress paths followed in conventional methods for the prediction of heave in one-dimension

This paper presents the results of analyses of a case history using a theoretically based method that can be used for the prediction of heave in one-, two- and three-dimensions. The method uses the input soil data from a one-dimensional oedometer test

(i.e., swelling index,  $C_s$  with swelling pressure; and/or swelling index,  $C_m$  with matric suction conditions).

### ***History of the study site and instrumentation***

In a program to study the performance of shallow foundation in expansive soils in western Canada, the Division of Building Research, National Research Council of Canada instrumented a typical single-story commercial building in north-central Regina, Saskatchewan. The building was placed on a perimeter beam supported by cast-in-place concrete piers. A concrete slab with a thickness of 100 mm was placed on a gravel fill layer of 180 mm over highly plastic clay. Construction of the building and instrumentation took place during the month of August 1961. Details on testing and monitoring programs were presented in Yoshida et al. (1983).

An auger boring was drilled and logged visually for the installation of the deep benchmark in August 1961. Shelby tube samples were taken at depths of 0.5, 1.2, 2.4, and 4.3 m from the original ground surface. Laboratory tests evaluated the Atterberg limits, *in situ* water content, grain-size distribution, swelling indices, and the corrected swelling pressures of the soil. On the average, the liquid limit was found to be 77%, with a plastic limit of 33% and natural water content of 29%. The specific gravity and unit weight for the soil profile were 2.82 and 18.88 kN/m<sup>3</sup>, respectively.

Constant volume oedometer tests on three samples were used to determine the initial void ratios, the swelling indices and the corrected swelling pressures. Table 1 presents the oedometer test results and water content of the samples. Although there was some variation in the initial void ratio and the swelling index, an average value of 0.962 for the initial void ratio and 0.090 for the swelling index will be used in the analyses. Figure 2 shows the distribution of the corrected swelling pressure with depth. A straight line can be used to represent the apparent distribution of the corrected swelling pressure with depth.

Table 1. Constant volume oedometer data (Yoshida et al. 1983)

Depth (m)	Initial void ratio, $e_0$	Swelling index, $C_s$	Corrected swelling pressure, $P'_s$ (kPa)
0.69	0.927	0.095	490
1.34	0.985	0.081	325
2.20	0.974	0.094	81

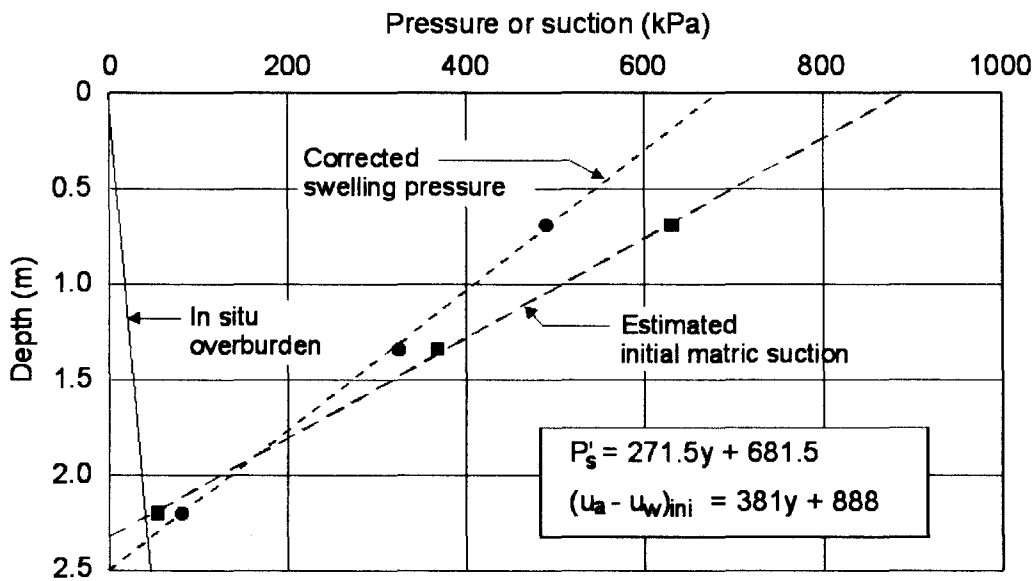


Figure 2. Distribution of corrected swelling pressure and estimated initial suction with depth.

Instrumentation installed at the site included a deep benchmark, ground movement gauges, and a neutron moisture meter access tube. The deep benchmark was installed at a depth of 16.8 m. Ground movement gauges were installed near the deep benchmark at depths of 0.88 m, 1.15 m, and 2.69 m below the design elevation of the floor slab. The neutron moisture tube was installed next to the ground movement gauges to a depth of 2.9 m; this tube allowed the monitoring of soil water contents adjacent to the tube without removing soil samples. Location of the instruments are shown in Figure 3.

Initial level readings were taken on August 23, 1961 on the ground movement gauges and on September 22, 1961 on the floor slab. Latter measurements of ground movements and water contents were taken about twice a year up to 1968, with additional measurements on ground movement gauges up to 1972. Level surveys of the floor slab were made in August 1962.

The building owner noticed heave and cracking of the floor slab in early August 1962, about a year after construction. The owner also noticed an unexpected increase in water consumption of approximately 35,000 L. The loss of water was traced to a leak in a hot-water line beneath the floor slab, which was subsequently repaired. The location of the cracking and contours of heave for the floor slab are showed in Figure 3.

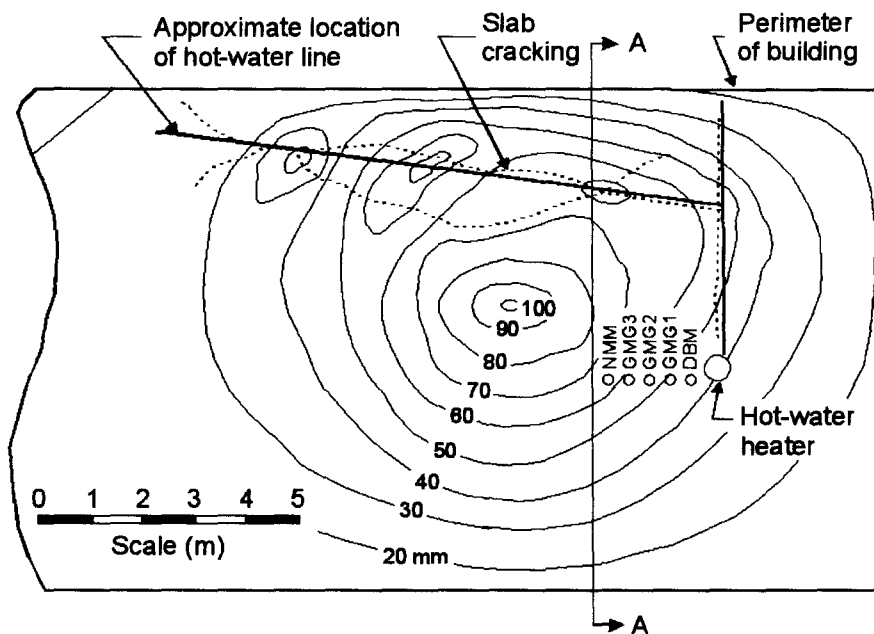


Figure 3. Floor plan of study site and contours of measured heave (NMM = neutron moisture meter; GMG = ground movement gauge; DBM = depth benchmark) (Yoshida et al., 1983)

### ***Method of analysis and Computer Program***

The analyses were performed for moisture movement and stress-deformation. The negative pore-water pressure (i.e., soil suctions) were estimated from a saturated-

unsaturated seepage analysis. The results were then used as input for the prediction of displacements in a stress-deformation analysis. The formulation of the governing partial differential equations for both seepage and stress-deformation are based on the general theory of unsaturated soils using two independent stress state variables (i.e, net normal stress and matric suction) and are presented in Vu and Fredlund (2000). A general-purpose partial differential equation solver, called FlexPDE<sup>1</sup> was used in this study to solve the saturated/unsaturated seepage and stress/deformation associated with the unsaturated soil. FlexPDE is a scripted finite element model builder and numerical solver that is capable of solving both two- and three-dimensional problems.

Two unsaturated soil properties are required when solving transient seepage problem; namely, the coefficient of water volume change (or coefficient of water storage), and the coefficient of permeability. Both the coefficient of water storage and the coefficient of permeability are predominantly functions of the matric suction. The solution for transient saturated-unsaturated seepage also requires the designation of initial soil suction conditions, as well as the moisture flux boundary conditions. The results of the seepage analysis provide the distributions of matric suction in the soil profile with respect to time for the specified boundary conditions.

The analysis of stress/deformation, under specified boundary conditions, requires the designation of initial matric suctions, initial stress conditions, the elasticity parameter functions associated with the volume change of the soil, and the results from a seepage analysis (i.e., for changes in soil suction). The elasticity parameter functions required for a stress-deformation analysis were calculated from conventional oedometer tests (Vu and Fredlund 2003).

### ***Characterization of the soil properties with the seepage analysis***

A seepage analysis was performed to predict changes in the matric suction condition in the soil. The initial matric suction conditions are estimated through the corrected swelling pressures. An approximate soil-water characteristic curve was defined using measured water contents at various values of soil suction.

The corrected swelling pressure is the sum of the overburden pressure and the matric suction equivalent and is written as follows (Fredlund and Rahardjo 1993):

$$[1] \quad P'_s = (\sigma_y - u_a)_{field} + (u_a - u_w)_e$$

where:

$P'_s$  = corrected swelling pressure,

$\sigma_y$  = original overburden pressure, and

$(u_a - u_w)_e$  = matric suction equivalent.

Initial matric suction conditions can be estimated from the corrected swelling pressure assuming a slope for the net normal stress versus matric suction curve at a constant void ratio (Figure 4). Let us assume that the slope can be written as a function,  $f$ , and for the sake of this case history, let the function be taken as equal to degree of saturation. Equation [1] then becomes:

$$[2] \quad P'_s = (\sigma_y - u_a)_{field} + f(u_a - u_w)_{field}$$

Therefore, the initial matric suction conditions required for the seepage analysis can be estimated as follows:

$$[3] \quad (u_a - u_w)_{field} = \frac{P'_s - (\sigma_y - u_a)_{field}}{f}$$

where:

$f$  = a function set equal to the degree of saturation.

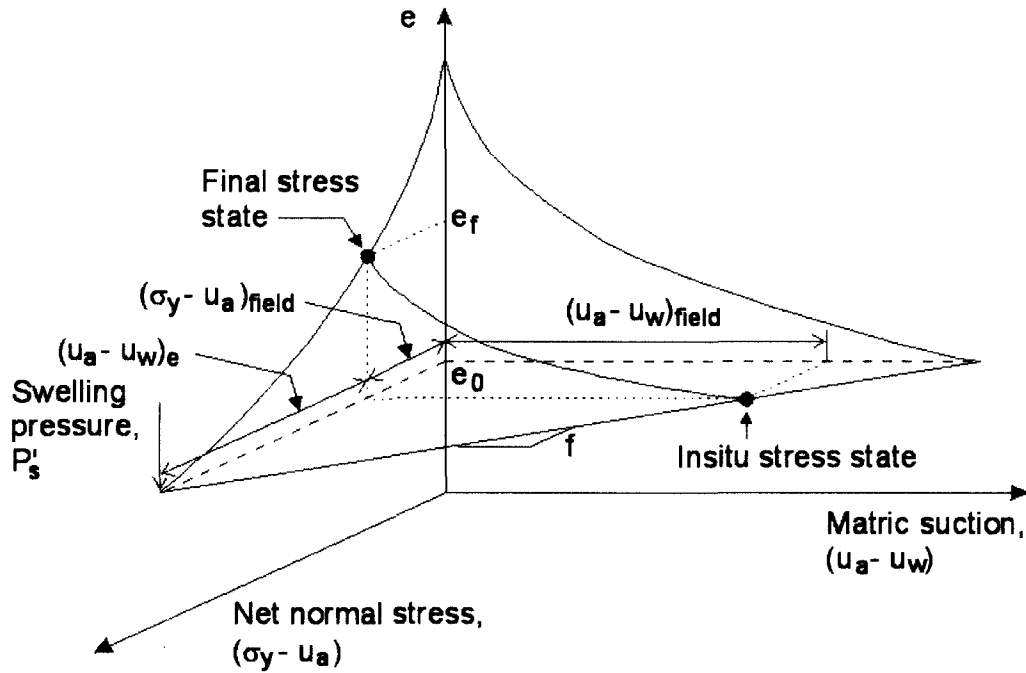


Figure 4. Assumed relationship between matric suction and matric suction equivalent

The estimation of initial matric suction condition is presented in Table 2 and shown graphically in Figure 2. A straight line can be used to represent the distribution of the initial matric suction with depth.

The initial degree of saturation and volumetric water content can also be calculated, since the initial water content profile has been established [i.e.,  $S = wG_s/e$  and  $\theta_w = wG_s/(1+e)$ ]. The measured data of water content, degree of saturation at various values of matric suction can be used to produce an estimated soil-water characteristic curve. The Fredlund and Xing (1994) equation for a soil-water characteristic curve with  $\theta_{sat} = 49.3\%$ ,  $a = 300$  kPa,  $n = 0.6$ , and  $m = 0.7$  was used to fit the volumetric water content data; and  $a = 300$  kPa,  $n = 0.5$ , and  $m = 0.7$  for the degree of saturation data. Figure 5 presents the volumetric water content versus soil suction curve and the degree of saturation versus soil suction curve.



Table 2. Estimation of initial matric suction from corrected swelling pressure

Variable	Depths (m)		
	0.69	1.34	2.20
Overburden pressure, $(\sigma_y \cdot u_a)_{ini}$ (kPa)	13.03	25.30	41.54
Initial void ratio, $e_0$	0.927	0.985	0.974
Corrected swelling pressure, $P'_s$ (kPa)	490	325	81
Gravimetric water content, $w$ (%)	25	29	31
Degree of saturation, $S$ (%)	76	83	90
Volumetric water content, $\theta_w$ (%)	36.6	41.2	44.3
Estimated field suction, $(u_a - u_w)_{ini}$ (kPa)	627	361	44

Note:  $S = wG_s/e$  and  $\theta_w = wG_s/(1+e)$

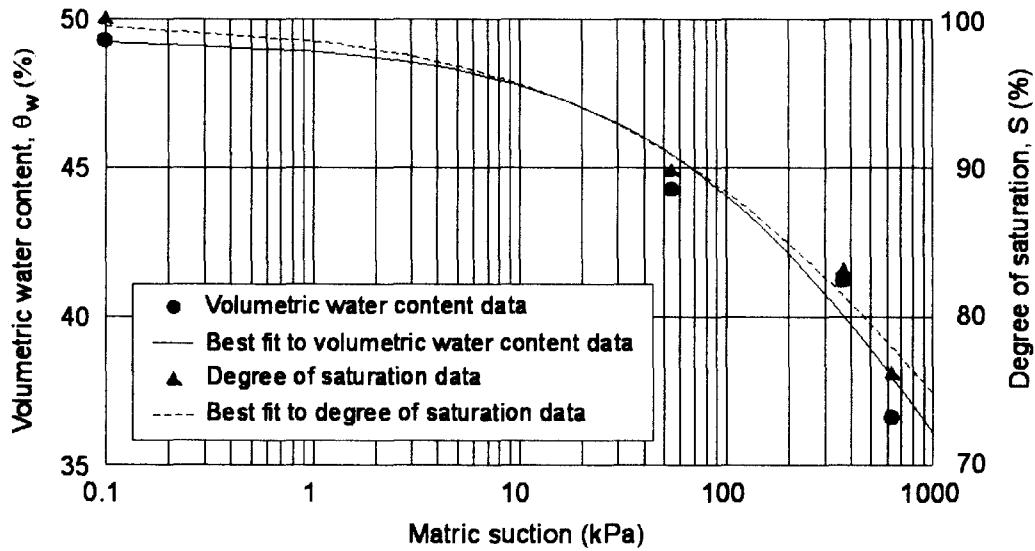


Figure 5. Estimated soil-water characteristic curve for Regina clay

A coefficient of permeability function for compacted Regina clay (Shuai 1996) was used for the analysis as part of this study. The coefficient of permeability function was described using the Leong and Rahardjo (1997) equation and presented graphically in Figure 6.

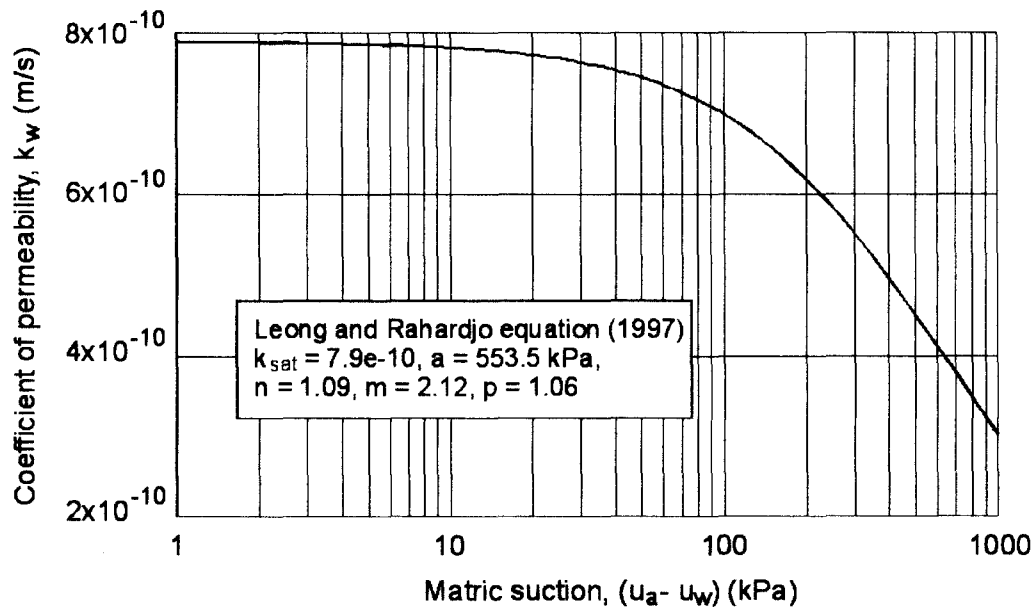


Figure 6. Computed coefficient of permeability function for Regina clay

The analysis examines the cross-section “A-A” shown in Figure 4. The lower boundary is selected at 2.3 m depth, where there was no apparent tendency for swelling (see Figure 2). This lower boundary can also be selected on the basis of the depth to which changes in matric suction appeared to be a minimum (Fredlund and Rahardjo 1993).

The geometry and boundary conditions for the seepage analysis is illustrated in Figure 7. It was assumed that water leaked from the water line along a 2 meters length of the line. It was assumed that the initial suction conditions did not change outside of the concrete slab and at the lower boundary. A moisture flux equal to zero was specified elsewhere along the boundaries. Matric suction conditions are predicted for various elapsed times (i.e., 5 days, 20 days, 50 days, 100 days and at steady state conditions).

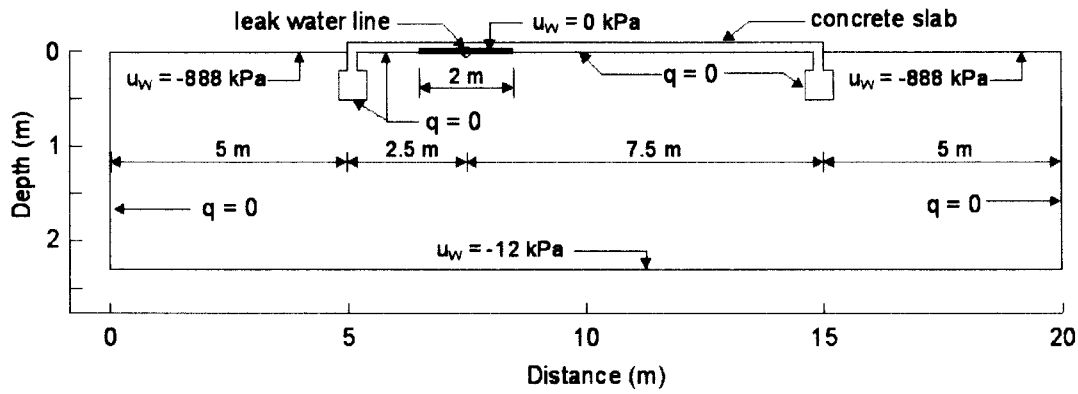


Figure 7. Geometry and boundary conditions for seepage analysis

### ***Characterization of the soil properties for the stress-deformation analysis***

Lytton (1994) presented typical values for coefficients of earth pressure at-rest,  $K_0$ , that were back calculated from field observations of heave and shrinkage. A coefficient of earth pressure equal to 0.667 was suggested for the case when the soil was wetting and cracks were closed. A Poisson's ratio equal to 0.40 was suggested from  $K_0$  using the following equation:

$$[4] \quad \mu = \frac{K_0}{1 + K_0}$$

The elasticity parameter function with respect to changes in net normal stress,  $E$ , can be calculated for two-dimensional condition (Vu and Fredlund 2003) for  $e_0 = 0.962$ ;  $C_s = 0.090$ ; and  $\mu = 0.40$  and can be written as follows:

$$[5] \quad E = \frac{4.605(1 + \mu)(1 - 2\mu)(1 + e_0)}{C_s} (\sigma_{ave} - u_a) = 28.11(\sigma_{ave} - u_a)$$

The swelling index with respect to changes in matric suction,  $C_m$ , was not measured for this case history. It is suggested that a value of  $C_s$  be used for  $C_m$ , and the initial stress state (*IST*) and final stress state (*FST*) from the net normal stress plane be used as the initial and final matric suctions for the stress-deformation analysis. The analysis procedure is illustrated in Figure 8.

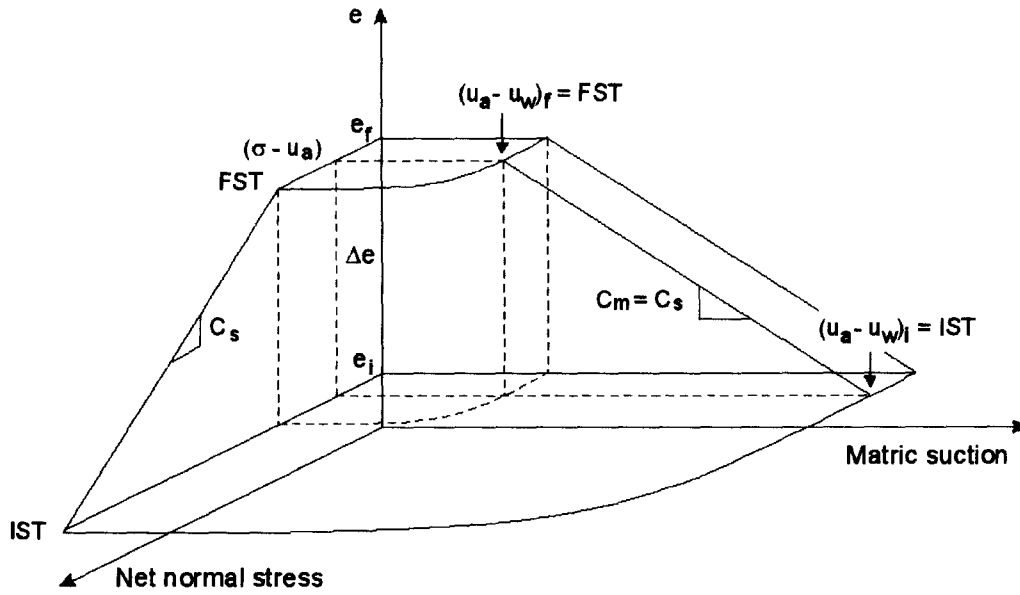


Figure 8. Illustration of the use of initial stress state (*IST*), final stress state (*FST*) and swelling index obtained at net normal stress plane ( $C_s$ ) for suction stress path

The elasticity parameter function with respect to changes in matric suction,  $H$ , can be calculated for two-dimensional condition (Vu and Fredlund 2003) for  $e_0 = 0.962$ ;  $C_m = 0.090$ ; and  $\mu = 0.40$  and can be written as follows:

$$[6] \quad H = \frac{4.605(1 + \mu)(1 + e_0)}{C_m} (u_a - u_w) = 140.5(u_a - u_w)$$

The *in situ* stress state (*IST*) is the sum of net normal stress and matric suction equivalent and can be written as follows for a two-dimensional analysis:

$$[7] \quad IST = (\sigma_{ave} - u_a)_i + f_i(u_a - u_w)_i$$

or

$$[8] \quad IST = \frac{1 + K_0}{2} (\sigma_y - u_a)_i + f_i(u_a - u_w)_i$$

The final stress state (*FST*) can be written as follows:

$$[9] \quad FST = (\sigma_{ave} - u_a)_f + f_f(u_a - u_w)_f$$

or

$$[10] \quad FST = \frac{1+K_0}{2}(\sigma_y - u_a)_i + \Delta(\sigma_{ave} - u_a) + f_f(u_a - u_w)_f$$

Deformation of the slab associated with this case was due to applied load and wetting. Deformation of the slab and in the soil mass due to loading can be assumed to respond immediately, while the deformations due to wetting are a time dependent process. Therefore, the stress-deformations due to loading and due to wetting need to be analyzed independently. Figure 9 shows the stress path followed in the analysis. The stress-deformation analysis was first performed to predict the displacements and induced stress due to the loading of the slab. The deformations due to changes in matric suction were then predicted for various elapsed times using matric suction profiles obtained from the seepage analysis. The stress-deformation analysis is also performed for the cases when pore-water pressure goes to zero and when the ground water level rises to ground surface resulting in a hydrostatic pore-water pressure distribution. Hydrostatic conditions present the upper limits for total heave.

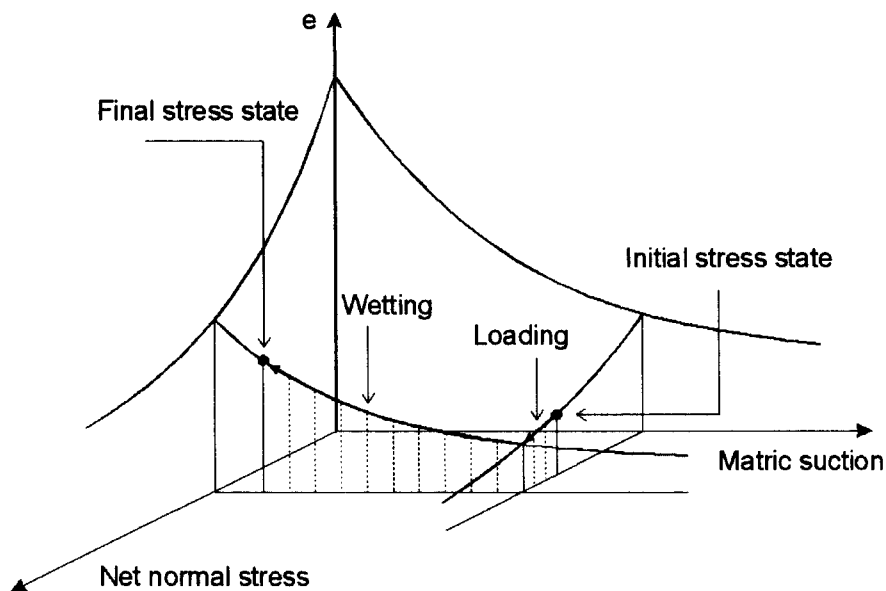


Figure 9. Stress path followed in the stress-deformation analysis

Figure 10 shows the geometry and boundary conditions for the stress-deformation analysis. A load equal to 5.76 kPa is applied on the surface of a 100 mm thick concrete slab. This surcharge is made up of 180 mm of fill with a unit weight of 18.88 kN/m<sup>3</sup> and 100 mm of concrete with a unit weight of 23.6 kN/m<sup>3</sup>. An accurate perimeter load is unknown, however, a typical value of 15 kN/m was assumed. The perimeter load includes the weight of footing and the load of the upper structure. The soil is free to move in a vertical direction and fixed in the horizontal direction at the left and right sides of the domain. The lower boundary is fixed in both directions. A Young's modulus of 10 GPa and Poisson's ratio of 0.15 was used for the concrete slab.

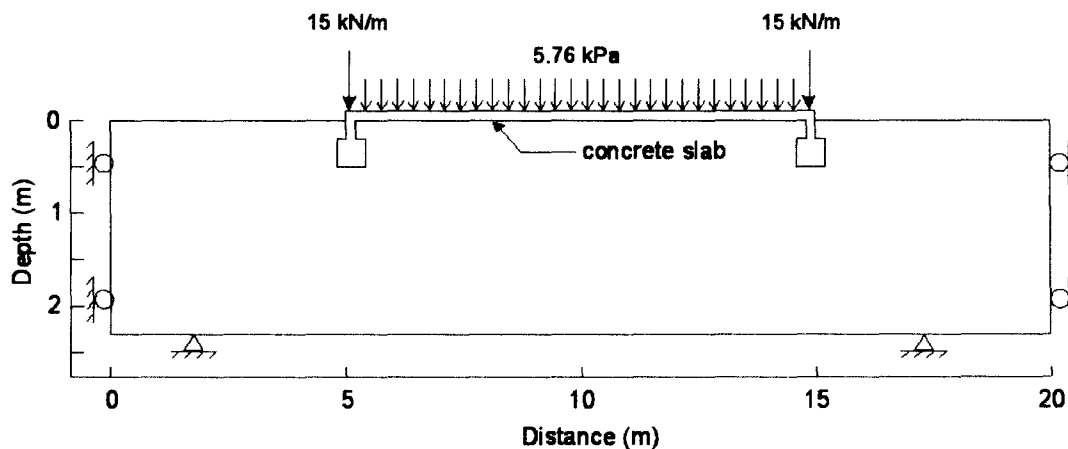


Figure 10. Boundary conditions for stress-deformation analysis

A parametric study was also performed to show the effect of varying Poisson's ratio, swelling index, initial void ratio, the coefficient of earth pressure at-rest, and the stiffness of the concrete slab on the predicted results.

### ***Computer results and discussions***

Figure 11 presents changes of matric suction with time at various points in the soil. Matric suctions decreased significantly during the first 30 days of wetting, and approached a steady state condition in about 150 days. The total amount of water that leaked from the water line with time is presented in Figure 12. A loss of 35 m<sup>3</sup> of water is

equivalent to approximately  $3.5 \text{ m}^3$  of water over each meter of the floor width. This amount of water is more than the amount of water required for the steady state condition attained under the specified boundary conditions. Figure 13 presents pore-water pressure profiles under the centre of the slab for various times and also for the case where the final pore-water pressure goes to zero and then a hydrostatic condition. Figure 14 shows the matric suction distribution in the soil at steady state conditions. It can be noted that under the specified boundary conditions, the matric suction at steady state conditions is about 20 kPa under the centre of the slab.

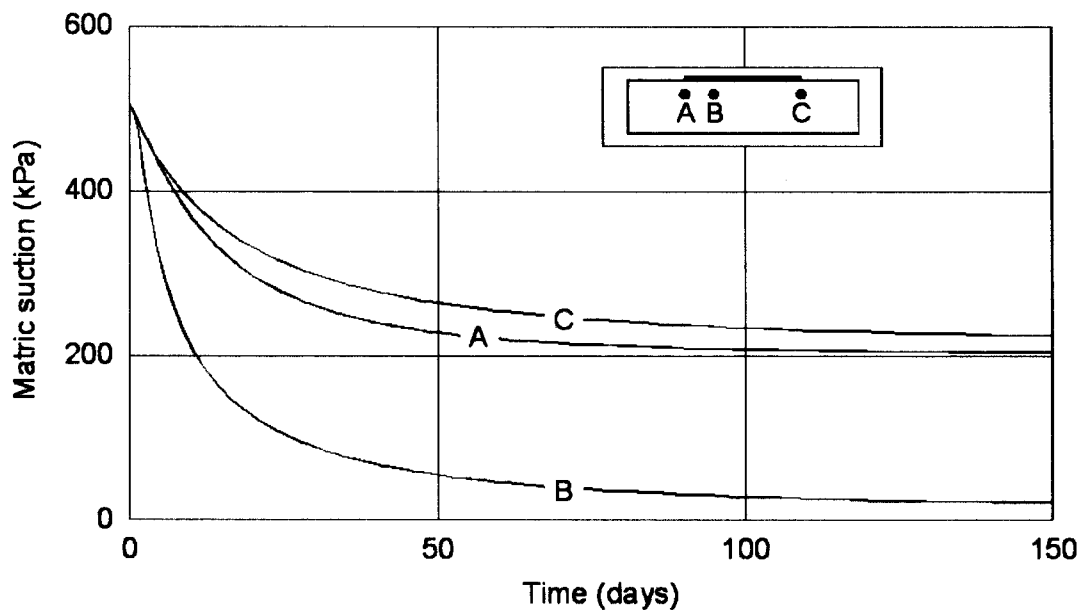


Figure 11. Matric suction changes with time for various point in the soil mass

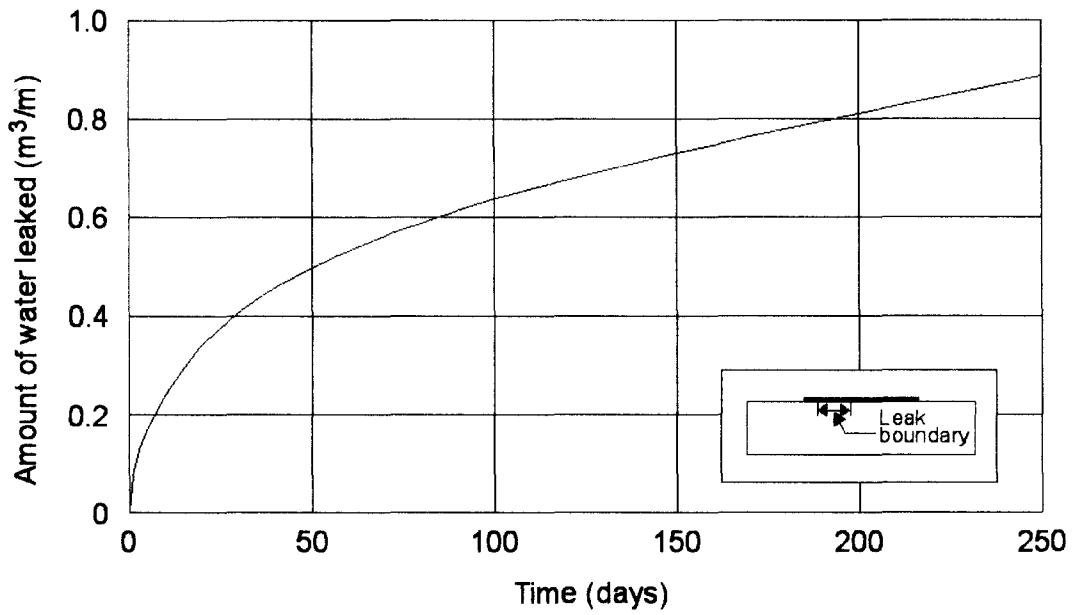


Figure 12. Total amount of water leaked from water line with time per meter of cross section

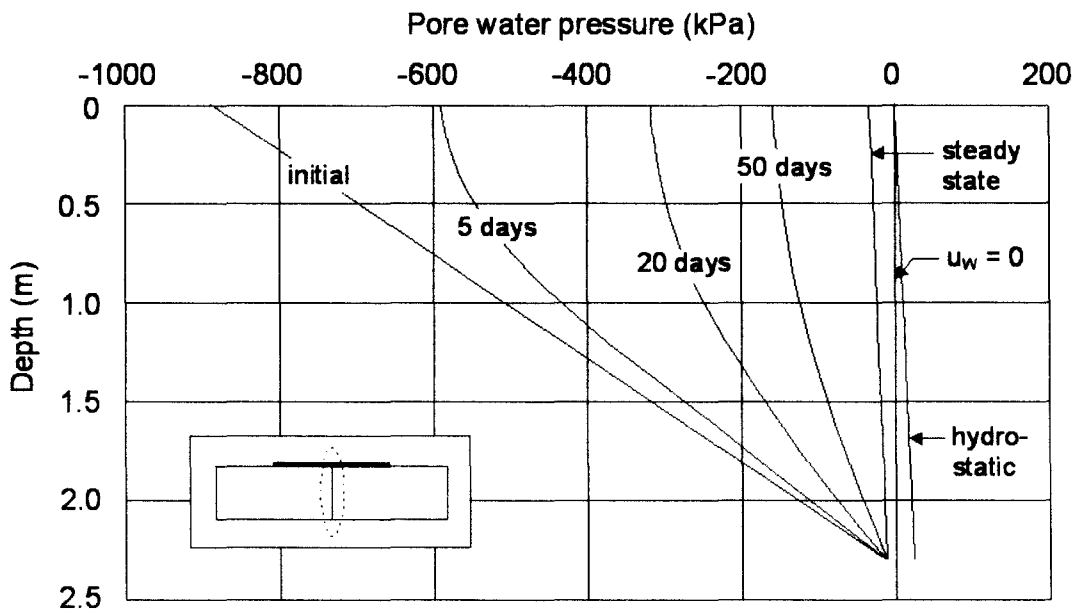


Figure 13. Pore-water pressure profiles for various times and for the cases where final pore-water pressure is assumed to be zero and hydrostatic



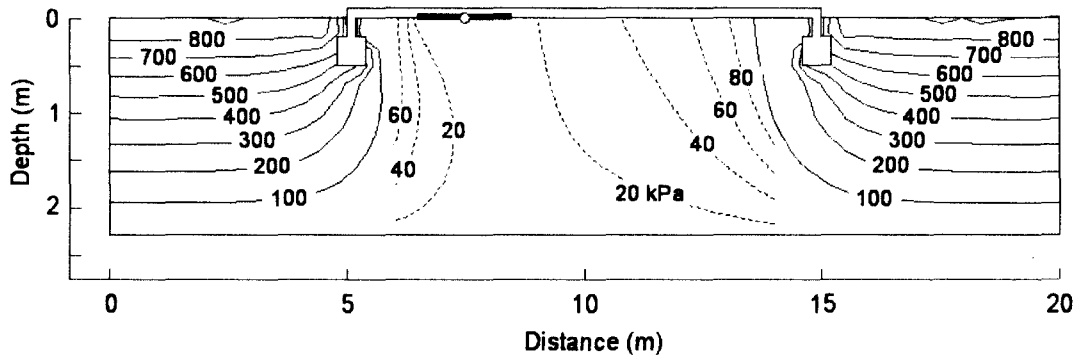


Figure 14. Matric suction distribution at steady state conditions

Figure 15 shows contours of vertical displacements due to loading. Less than 1 mm of settlement is predicted due to the loading at the centre of the slab. The induced net normal stress was used to calculate the final net normal stress state in the soil. Also, the soil was loaded at initial net normal stress and matric suction conditions in the field. Therefore, the sum of initial net normal stress and initial matric suction equivalent must be used along with the swelling index obtained on the net normal stress plane for the prediction of displacements and induced stresses due to loading.

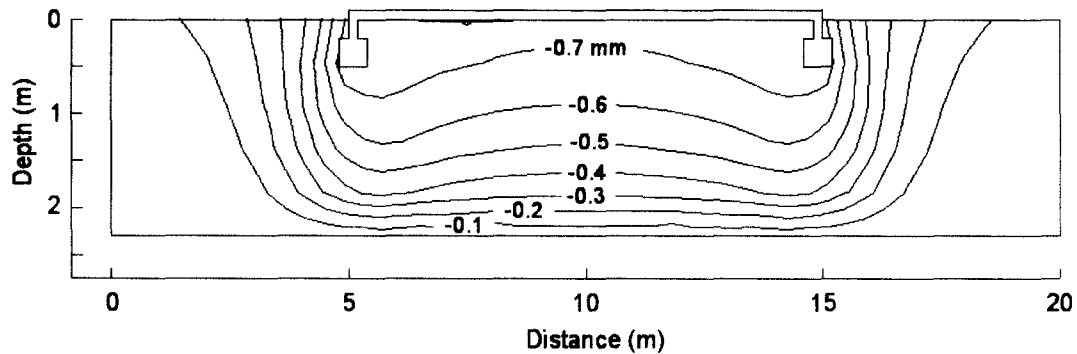


Figure 15. Distribution of vertical displacements due to loading

Figure 16 compares the predicted vertical displacements at various final suction conditions with the measured total heave at the centre of the slab. The agreement between the predicted and the measured heave at different depths differ to some degree. The amounts of heave measured at depths of 0.58 and 0.85 m correspond to the predicted heave at 100 days, while the total heave of 106 mm at ground surface corresponds to the case when the pore-water pressure goes to zero under the slab. It must be noted that a heave of 106 mm represents the maximum heave observed on the slab. The maximum heave observed at the cross-section under consideration is only 80 mm (see Figure 3). The distribution of horizontal displacements at different final suction conditions right under the water line is presented in Figure 17.

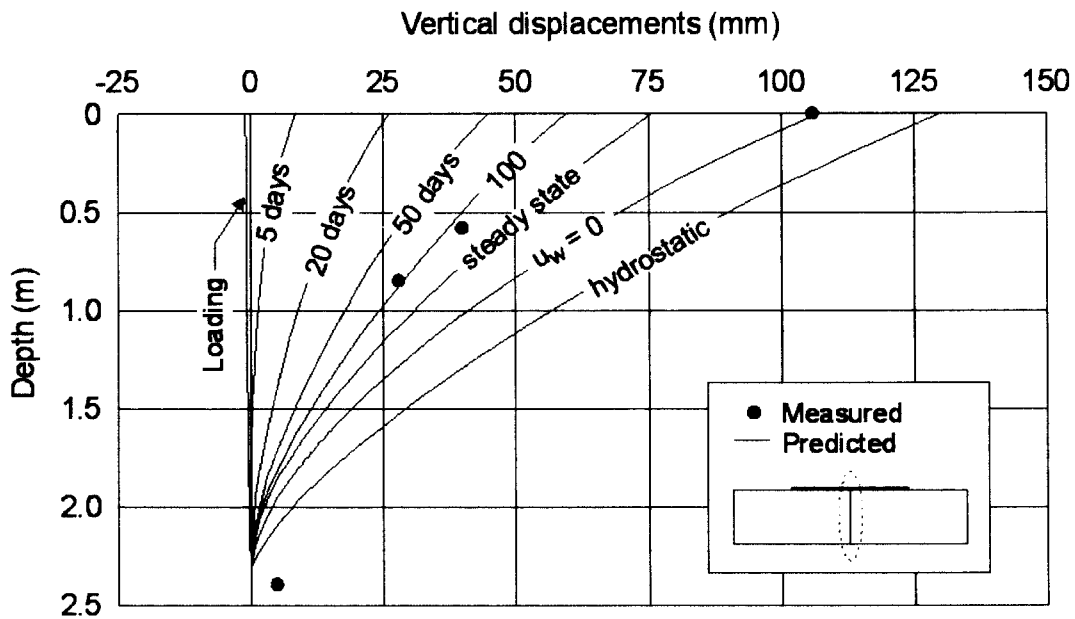


Figure 16. Measured and predicted vertical displacements with depth near the center of slab

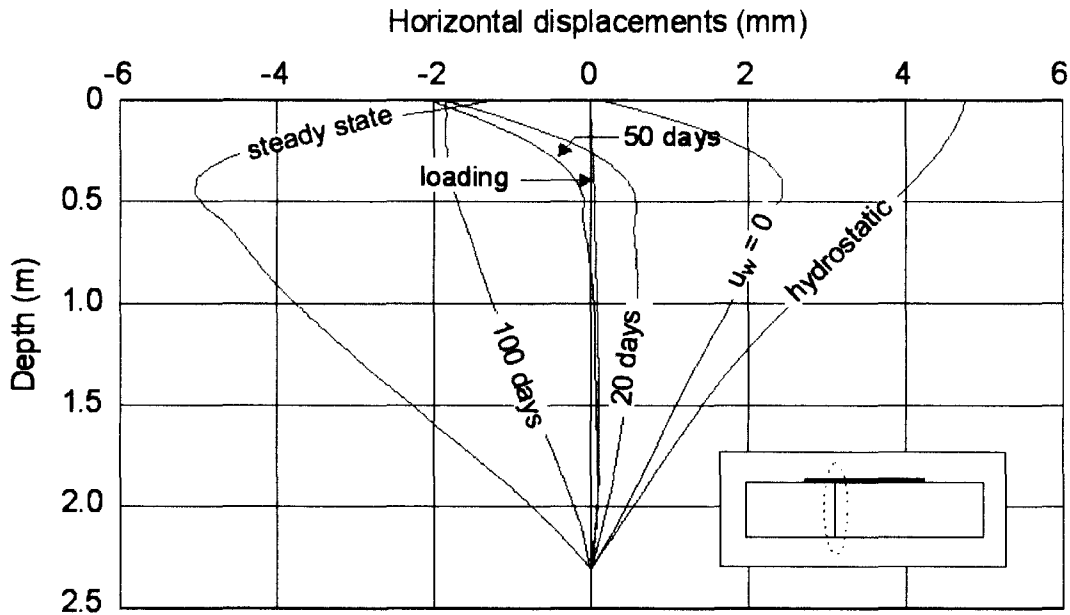


Figure 17. Distribution of horizontal displacements with depth at different suction conditions under the water line

Figure 18 compares the predicted vertical displacement at various final matric suction conditions with the measured total heave at the top surface of the slab. The total heave predicted under steady state conditions agrees well with the measured heave. It should be noted that there were some unknown loads placed near the perimeter of the floor slab and this was not considered in the study. Assuming that the final pore-water pressure increases from a negative value to zero results in a maximum predicted heave of 107 mm. A maximum heave of 130 mm is predicted for the case when the final pore-water pressures are assumed to be hydrostatic.

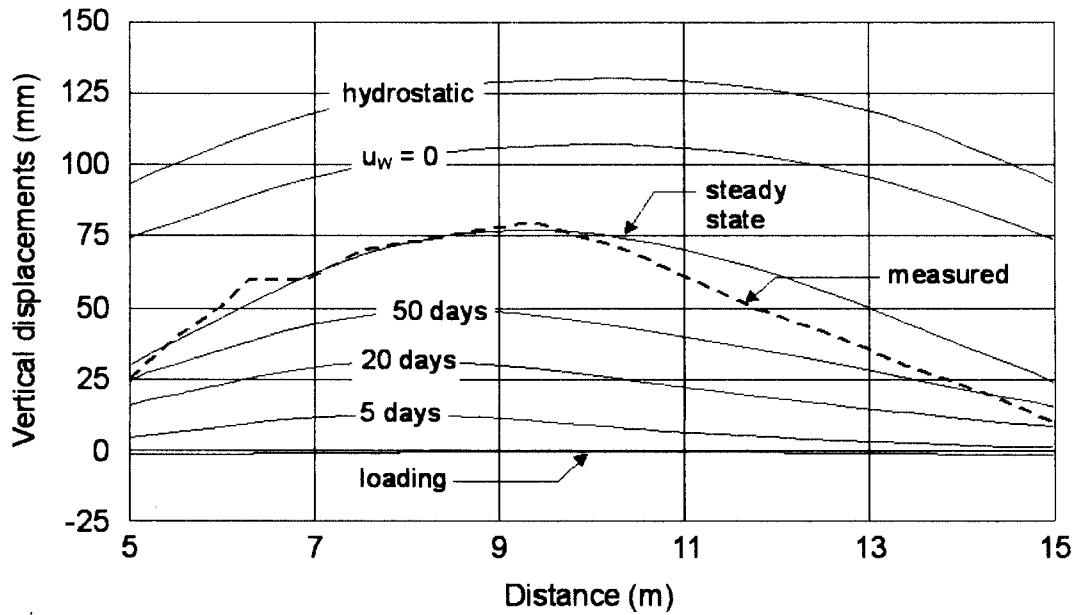


Figure 18. Measured and predicted vertical displacements at surface of the slab

Figure 19 shows the measured and predicted water contents under the center of the slab. The final water contents predicted at steady state conditions is about 3% less than the measured final water contents. When the pore-water pressure increased to zero, the predicted final water content is about 2% more than the measured values. The distribution of water contents and vertical displacements in the soil predicted at steady state conditions is showed in Figures 20 and 22, respectively.

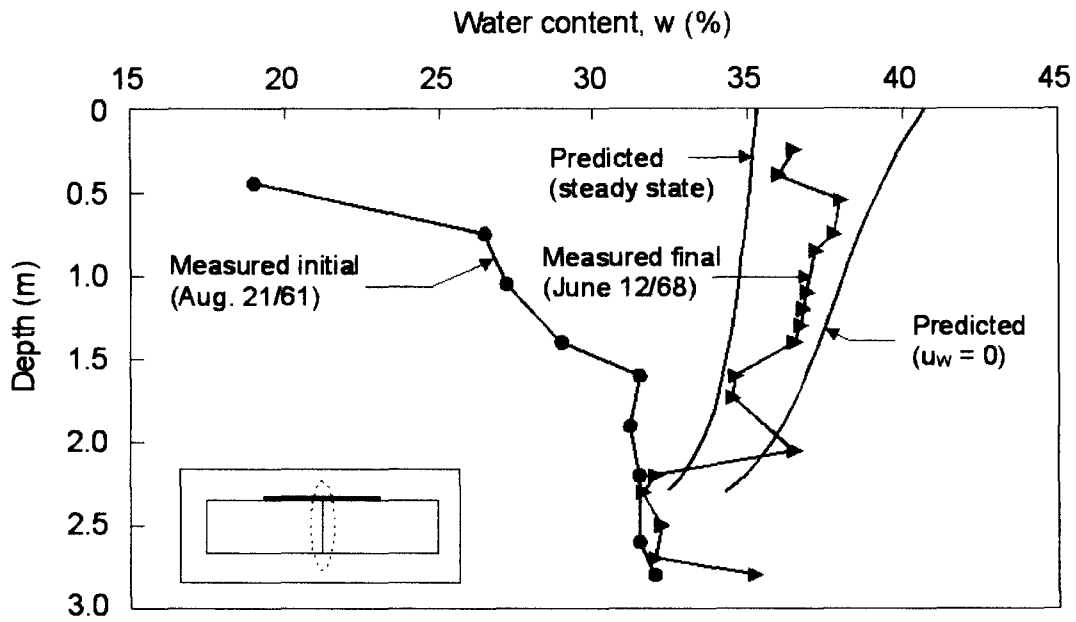


Figure 19. Measured and predicted water content with depth near the center of slab

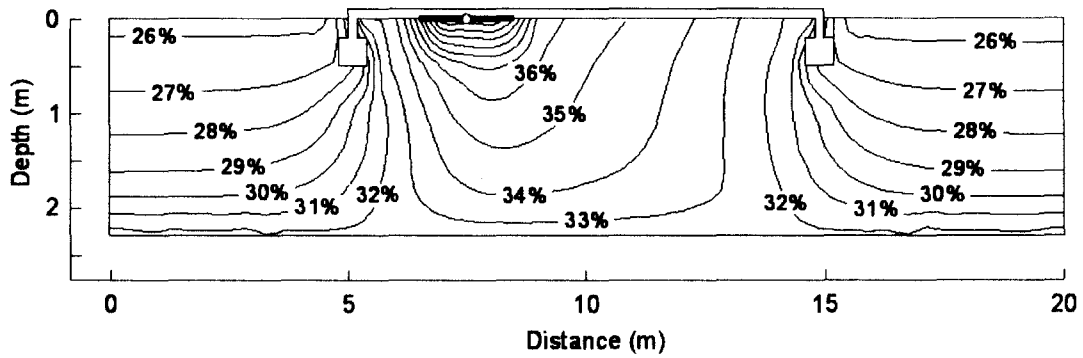


Figure 20. Distribution of gravimetric water content at steady state conditions

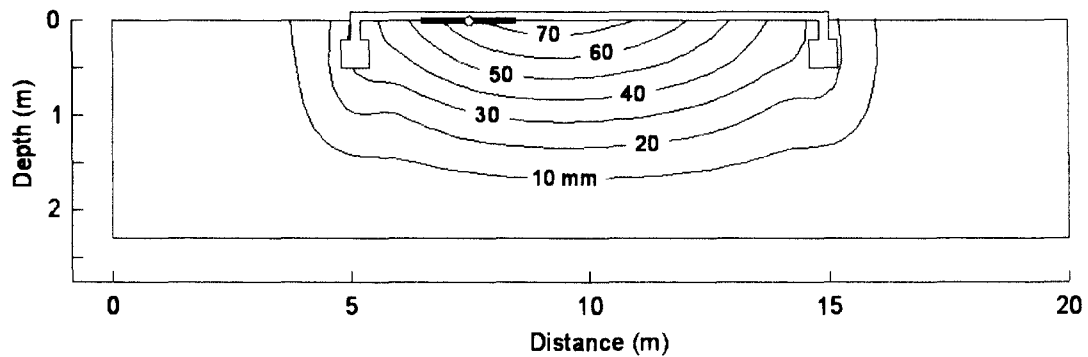


Figure 21. Distribution of vertical displacements at steady state conditions

### ***Results of the parametric studies***

The results of the above-presented stress-deformation analysis depend on the calculated elasticity parameter functions (i.e.,  $E$ ,  $H$ , and  $\mu$ ), initial stress state conditions and the stiffness of the concrete slab. The elasticity parameters,  $E$  and  $H$ , are calculated from the initial void ratio,  $e_0$ , swelling index,  $C_s$ , and the assumed value of Poisson's ratio,  $\mu$ . The initial horizontal net normal stress is estimated using the coefficient of earth pressure at-rest,  $K_0$ .

Several stress-deformation analyses were performed to study the effect of each of the above parameters on the solutions and to gain confidence in their significance to the analysis. For each case, only the parameter under consideration was allowed to vary, all other parameters were kept unchanged at the values used for the "base case". Table 3 shows the values of the parameters that were used in the parametric study. It should be noted that the relationship between Poisson's ratio and the coefficient of earth pressure at-rest (i.e., Eq. [4]) was not considered in the parametric studies. The displacements are only calculated for steady state conditions of matric suction. The results of the parametric study are summarized in Table 4. It can be seen that swelling index and Poisson's ratio are the factors that have the greatest effect the solution. The value of Young's modulus for concrete appears to control the shape of deformed slab.

Table 3. Values of parameters used in parametric study

Parameter	Lower values	Base case	Upper values
Poisson's ratio, $\mu$	0.30, 0.35	0.40	0.45, 0.49
Swelling index, $C_s$	0.085	0.090	0.095, 0.100
Initial void ratio, $e_0$	0.920	0.962	1.000
Coefficient of earth pressure at-rest, $K_0$	0.400	0.667	1.000
Young modulus of concrete, $E_c$ (GPa)	5	10	20

Table 4. Results of parametric study

Parameter	Range	Variation of predicted heave (%)
Poisson's ratio, $\mu$	0.35 - 0.45	$\pm 7$
Swelling index, $C_s$	0.085 - 0.95	$\pm 5$
Initial void ratio, $e_0$	0.92 - 1.00	$\pm 2$
Coefficient of earth pressure at-rest, $K_0$	0.4 - 1.0	$\pm 2$
Young modulus of concrete, $E_c$ (GPa)	5 - 20	$\pm 3$

### ***Conclusions***

The method for the prediction of multi-dimensional heave based on the general theory of unsaturated soil, expansive soils was verified using data collected for the case history of a floor slab in a light industrial building on Regina clay. Changes in matric suction (or pore-water pressure) in the soil mass are estimated through a saturated-unsaturated seepage analysis. Displacements due to loading and changes in matric suction are predicted using a stress-deformation analysis. The required elasticity parameter functions required for the stress-deformation analysis can be calculated from conventional oedometer test results. The predicted results appear to be in reasonable agreement with measured values. The predicted heave is somewhat sensitive to the assumed value of Poisson's ratio and the measured swelling index and insignificantly affected by the initial void ratio measured in the laboratory and the coefficient of earth pressure at-rest.

### ***Reference***

- Fredlund, D.G. and Rahardjo, H. 1993. Soil mechanics for unsaturated soils. John Wiley & Sons, New York, 560 p.
- Fredlund, D.G. and Xing, A. 1994. Equation for the soil-water characteristic curve. Canadian Geotechnical Journal, **31**(3): 521-532.
- Jaky, J. 1944. The coefficient of earth pressure at rest. Journal of the Society of Hungarian Architects and Engineers, **78**(22): 355-358.

- Leong, E.C. and Rahardjo, H. 1997. Permeability functions for unsaturated soils. *Journal of Geotechnical and Geoenvironmental Engineering*, ASCE, pp: 1118-1126.
- Lytton, R.L. 1994. Prediction of movement in expansive clay. Vertical and horizontal deformations of foundation and embankments, *Geotechnical Special Publication*, ASCE, New York, **40**(2): 1827-1845.
- Shuai F. 1996. Simulation of Swelling Pressure Measurements on Expansive Soils. Ph.D. dissertation, University of Saskatchewan, Saskatoon, 228 p.
- Vu, H.Q. and Fredlund D.G. 2000. Volume Change Predictions in Expansive Soils Using a Two-dimensional Finite Element Method. *Proceeding, Asian Conference on Unsaturated Soils*, Singapore, pp. 231-236.
- Vu, H.Q. and Fredlund D.G. 2003. Implementation of Soil Property Functions in Volume Change Analysis in Unsaturated Soils. *Proceeding, 12th Asian Regional Conference (12ARC)*, Singapore.
- Yoshida, R.T, Fredlund, D.G., and Hamilton, J.J. 1983. The prediction of total heave of a slab-on-grade floor on Regina clay. *Canadian Geotechnical Journal*, **20**: 69-81.
- <sup>1</sup>FlexPDE is a proprietary product of PDE Solutions Inc., 2120 Spruce Way, Antioch, CA 94509, USA